IEEE Access
Multidisciplinary ⋮ Rapid Review ⋮ Open Access Journal

Received February 1, 2021, accepted February 16, 2021, date of publication February 23, 2021, date of current version March 25, 2021.

Digital Object Identifier 10.1109/ACCESS.2021.3061552

Rock Strength Determination Based on Rock Drillability Index and Drilling Specific Energy: Numerical Simulation Using Discrete Element Method

BOSONG YU, KAI ZHANG, AND GANGGANG NIU

State Key Laboratory for Geomechanics and Deep Underground Engineering, China University of Mining and Technology, Xuzhou 221116, China
School of Mechanics and Civil Engineering, China University of Mining and Technology, Xuzhou 221116, China

Corresponding author: Kai Zhang (kzhang@cumt.edu.cn)

This work was supported by the National Natural Science Foundation of China under Grant 52074260.

ABSTRACT In the present research, two real-time rock strength determination models based on the drilling parameters were studied. Firstly, a discrete element software named Particle Flow Code in 2 Dimensions (PFC^{2D}) was used to analyze the applicability of rock drillability index and drilling specific energy, in which graded particle assemblies were created to simulate the rock behaviour. In the numerical models, Weibull distribution was used to randomize the bonds between particles and make the assembled rock model with different heterogeneity. The drilling process of a PDC (polycrystalline diamond compact) cutter was modelled in two steps: horizontal linear rock cutting and vertical pressing-in progress. From the horizontal linear rock cutting process, the peak cutting forces were obtained and vertical pressing-in process outputs the relationship between normal force and cutting depth. Subsequently, the methods for calculating rock drillability index and drilling specific energy were proposed in the discrete element model. Then, the relationship between the calculated indexes and rock strength was investigated (supported with the regression analysis). Moreover, the effect of rock heterogeneity, along with error comparison between the above two indexes, were discussed. The results showed that the rock drillability index is more accurate than drilling specific energy in rock strength assessment (The error is about 10% smaller).

INDEX TERMS Rock drillability index, drilling specific energy, heterogeneity, discrete element method, cutting force.

I. INTRODUCTION

The information about the surrounding rock's geological conditions plays a vital role in the design of the support of the coal mine roadways. There are currently many methods to detect geological conditions, such as geological radar, electrical survey system, and advanced drilling technology. [1]–[8]. The most commonly used method for detecting the geological conditions in the geoengineering is advanced drilling technology which can easily obtain the core, making it the most direct and accurate geological prediction method. However, advanced drilling technology does not have a high core extraction rate under poor geological conditions, which lead to a certain degree of unreliability. In addition, the core extraction process takes too much time and costs, which severely affects the construction process and efficiency. On the other hand, geological radar and electrical survey system are indirect methods to detect the geological conditions. They are limited by underground observation conditions and the influence of the roadway environment, making them have the disadvantage of multi-solution. Therefore, their detection accuracy needs to be further improved. Zhang *et al.* proposed a rock drillability index based on MWD (measurement while drilling) method, which can be used to assess the geological conditions [9]. Meanwhile, Teale suggested using drilling parameters to calculate the drilling specific energy. This calculation method based on energy conservation defines the energy required to excavate the unit volume of rock [10]. In the present study, the applicability of the two methods will be discussed by numerical modelling.

The associate editor coordinating the review of this manuscript and approving it for publication was Lefei Zhang.

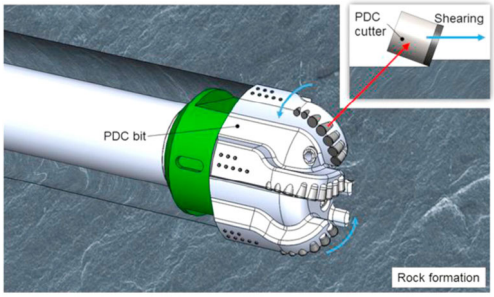

FIGURE 1. Rock drilling performed by a PDC cutter [21].

As shown in **Figure 1**, it is a typical PDC cutter used in coal mines. It is complicated to simulate the rock breaking process by the entire drill bit. Therefore, this research mainly focuses on a single PDC cutter. Meanwhile, understanding the mechanical mechanism in rock breaking by single PDC cutter plays a critical role in the numerical simulation of this study.

In the light of the above, in this work, a novel numerical simulation model will be made which is aimed at verifying rock drillability index and drilling specific energy (The newly derived formulas were introduced in this study to make these two methods capable for single PDC cutter) from a mechanical point of view. This work fills the major gap in the rock strength assessment since no researchers have analyzed the applicability of the above two methods by using a single PDC cutter. But, before going into the numerical simulation and theory, a literature review is given to introduce the huge efforts done in the study of horizontal linear rock cutting and vertical rock pressing-in by the single PDC cutter in the past and explain the rationale for the approach proposed in this study.

In the last few decades, many scholars explained the rock removal mechanism in various ways. Currently, there are two main failure modes widely recognized in rock cutting theory: crushing and chipping modes [11]. In the process of PDC rock cutting, the failure of the rock is an extremely complex fracture process. Although many scholars have studied the basic mechanism, a clear consensus has not yet reached. Some researchers have proposed that the failure of the rock during rock cutting is caused by tensile fracture [12]–[15], while others believe that shear failure is the internal cause [16]–[20]. The indoor rock cutting test is the most reliable and effective method to observe the interaction between the PDC cutter and the rock, and obtain the force acting on the cutter. At present, some scholars have conducted a series of indoor rock cutting tests [21], [22].

Although many methods are mentioned above to analyze the force acting on the PDC cutter, the numerical simulation is a more convenient method [23]–[28]. The 2-D discrete element simulation software (PFC^{2D}) is one of the effective tools for simulating rock mechanical behaviour in the engineering field since it can assign various combination conditions to the model, including faults, discontinuities and cracks [29]–[32]. Moreover, it can also simulate processes such as rock damage, chip formation and crack propagation.

In this study, at first, the force acting on the PDC cutter is introduced during horizontal linear rock cutting from a theoretical perspective. Then, the processes of horizontal linear rock cutting and vertical rock pressing-in are analyzed, which provide a theoretical basis for modelling in the numerical simulation. According to the theoretical basis, this work carried out numerical modelling and calculation for rock cutting and pressing-in tests in PFC^{2D}, which can verify the reliability of rock drillability index and drilling specific energy. On the other hand, this work studied the influence of heterogeneity on the applicability of rock drillability index and drilling specific energy by simulating the cutting of rocks with different heterogeneity, which provides a reliable basis for the wide application of these two rock strength assessment methods.

II. THEORY OF ROCK BREAKING BY PDC CUTTER

This section will give a brief introduction of the force condition in the horizontal linear rock cutting with a single PDC cutter and then state the theory of horizontal linear rock cutting and pressing-in processes, which provide theoretical support for the subsequent modelling work.

A. MODEL OF CUTTING WITH A SINGLE PDC CUTTER

In the actual drilling process, the PDC cutter is pressed into and cuts the rock obliquely. It should be noted that during the drilling process, the resultant force acting on the single PDC cutter can be divided into three orthogonal force: normal force (perpendicular to cutting direction), cutting force (parallel to cutting direction) and side force (transverse to cutting direction). Cutting force and normal force play a significant role in the rock drillability index and drilling specific energy. In contrast, side force is quite small and not taken into consideration by this study [33]. Therefore, this work divided the drilling process into two separate processes: horizontal linear rock cutting and vertical rock pressing-in [34]. The horizontal linear rock cutting process can be described as a phenomenon in which the PDC cutter moves parallel to the free surface of the rock and scrapes a part of the rock chip. Without considering the wear of the cutter, this process can be considered as a pure cutting process that occurs on the cutting face. Meanwhile, the vertical rock pressing-in process can be described as the phenomenon that the PDC cutter moves perpendicular to the free face of the rock and crushes the rock. The first rock cutting model is a semi-empirical model based on Moore Coulomb's plasticity criterion, and it considers the force balance of a single shear surface under orthogonal cutting. This model is suitable for rock cutting and can be well adapted to the cutting process of perfect sharp cutters without considering wear [35], [36]. Detournay and Defourny proposed a new cutting model (called the D-D model) in 1992. They believed that the force acting on a single PDC cutter is the coexistence of two independent processes:

'pure cutting' in front of cutting face and 'friction contact' in wear plane [37].

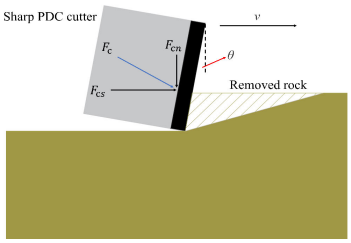

FIGURE 2. Forces acting on a sharp PDC cutter [39].

To study the cutting process without considering wear, a perfectly sharp cutter is proposed in **Figure 2**. According to the D-D model, without wearing, the resultant force acting on the PDC cutter is only the cutting force, that is, the process is a pure cutting process [38]. So, cutting force can be decomposed into the component form: normal component F_{cn} and tangential component F_{cs}. Since this study sets the back angle of the PDC cutter to 20°, the normal component of the cutting force acting on the cutter is negligible compared with the actual pushing force during drilling. Therefore, only the tangential component of the cutting force is collected.

B. ANALYSIS OF ROCK BREAKING PROCESS

Rock breaking theory during horizontal linear rock cutting and vertical rock pressing-in is introduced in this section, which provides a basis for modelling in the numerical simulation. As shown in **Figure 3**, the spalling of rock chip by cutting is a cyclic process in the process of continuous horizontal linear rock cutting [34]. As illustrated in **Figure 3(a)**, the PDC cutter breaks the rock under the action of horizontal speed. When the cutter just touches the rock, the load is relatively small. At this time, the rock contacting with the PDC cutter reaches the limit state, resulting in partial cracks. As the load increases, part of the rock is peeled off from the virgin rock under tensile stress. Due to the effect of confining pressure, the peeling surface will not develop to the deep rock mass without deep natural fractures, but to the free surface, as shown in **Figure 3(b)**, and this process will also cause small shear cracks on the peeling surface. As the cutting process continues, the rock chips are discharged. Simultaneously, the cutter continues to cut the rock below the peeling surface, as shown in **Figure 3(c)**, which make the reaction force of cutter on the rock suddenly decrease to a small value. After the rock below the peeling surface is eliminated, the PDC cutter will contact the rock again, and the above process will be repeated many times during the whole cutting process. However, the torque is almost stable in the actual drilling process, and it can be considered that the process of **Figure 3(a)** and **Figure 3(c)** is short and can be ignored. So, this study proposes that the cutting force obtained in the numerical simulation should be the force required by the cutter to peel a complete rock block from the virgin rock, that is, the peak cutting force in the process of **Figure 3(b)**.

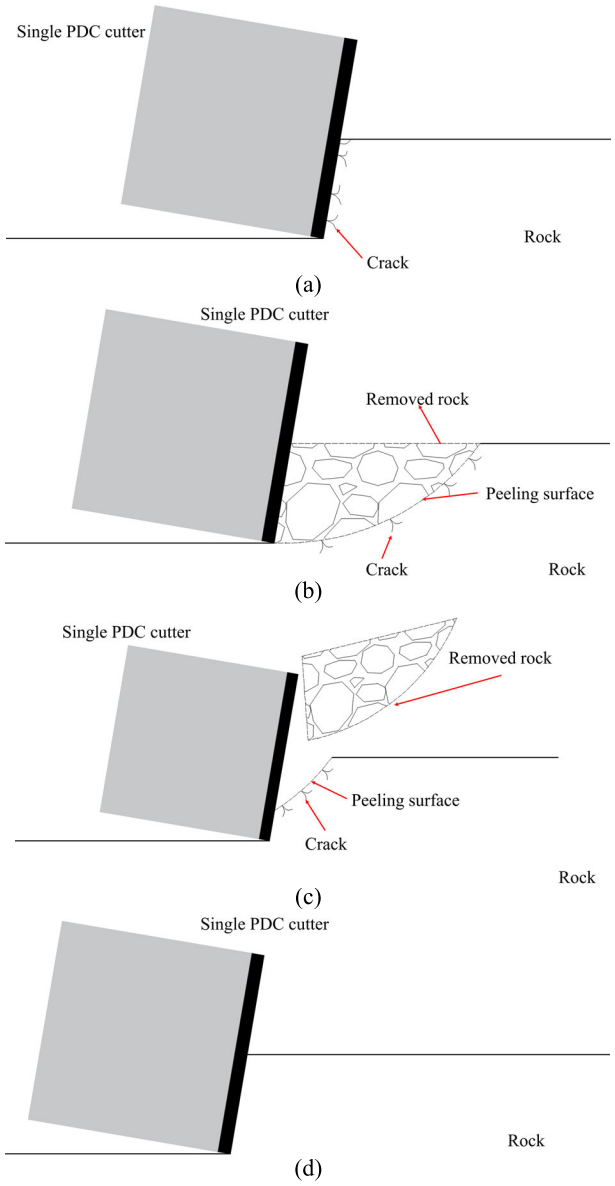

FIGURE 3. Process of rock breakage and crack development during horizontal linear rock cutting [34].

On the other hand, the vertical rock pressing-in is also a cyclic process [34]. As shown in **Figure 4**, the PDC cutter is pressed into the rock under the action of the vertical load. When the PDC cutter contacts the rock, the rock at the edge of the cutter will quickly reach the limit state. After the PDC cutter pressed into the rock to a small depth, there is a certain contact area between the cutter and the rock, which cause an increment of pressing force when cutter continues to press-in deeper. As the pressing force continues to increase, as illustrated in **Figure 4(b)**, the compacted rock chip will form below the left and right sides of the PDC cutter. When the pressing force is further increased, the rock on both sides of the PDC cutter will have cracks that will develop to the free surface of the virgin rock, and the crushed rock on both sides of the cutter will be discharged, as shown in **Figure 4(c)**,

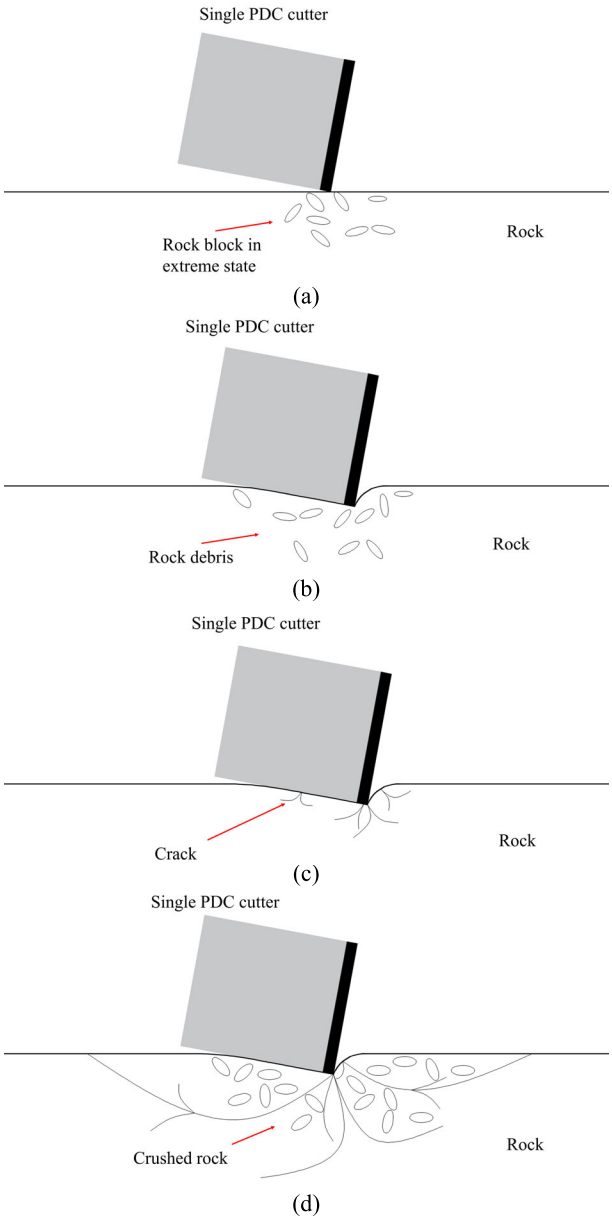

FIGURE 4. Process of rock breakage and crack development during vertical rock pressing-in [34].

which causes a sudden reduction in the force between the cutter and the rock. As the pressing process continues, the PDC cutter will be pressed further into the rock, and in a certain depth, the cutter is in close contact with the rock again, which makes the above pressing-in process repeated.

III. NUMERICAL MODEL

In this section, models of horizontal linear rock cutting and vertical rock pressing-in have been established and calibrated to predict the relationship between rock drillability index, drilling specific energy and rock strength. The horizontal linear rock cutting test reveals the cutting force required for the cutter to break the rock, and the rock pressing-in test analyzes the change of normal force acting on the cutter with the cutting depth.

A. SIMULATION SOFTWARE OVERVIEW

Simulation of particle motion behaviour is significant progress in the field of geotechnical engineering. 2-D particle flow can be modelled by the computer program, which is widely used in rock and soil mechanics, structural analysis and other fields. At present, the discrete element method (DEM) is generally used to simulate the motion and contact of rigid spherical particles. Cundall proposed to use the discrete element method to model and analyze rock mechanics problems [40], and then this method is applied to solve soil mechanics problems by Cundall and Strack [41].

Since horizontal linear rock cutting by a single PDC cutter can be regarded as a plane stress problem, this study uses PFC^{2D} to model and analyze the rock cutting and rock pressing-in. PFC^{2D} software has excellent effect on the simulation of rock mechanics and rock cutting process. The model particles are rigid bodies with normal and tangential stiffness, which are represented by disks with unit thickness in PFC^{2D}. There are two bonding methods between particles which are suitable for simulating rock, as shown in **Figure 5**, namely contact bonds and parallel bonds. Contact bonds can only reflect the normal and tangential force (action) between particles, while parallel bond can transmit force and moment. To fully characterize the mechanical properties of the rock, this study uses both types of bands [42].

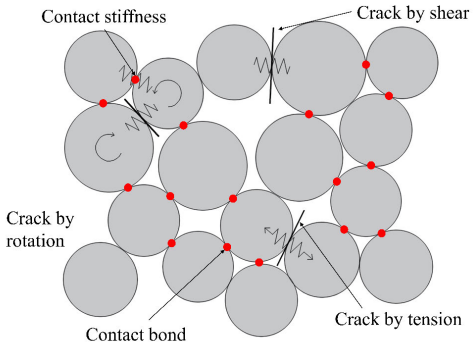

FIGURE 5. Cohesive model and its micro-mechanical behaviour schematic diagram. [43], [44].

B. ESTABLISHMENT OF THE ROCK CUTTING AND ROCK PRESSING-IN MODEL

The model established in this work is divided into two parts: models of horizontal linear rock cutting and vertical rock pressing-in. Horizontal linear rock cutting tests will be introduced first, which contain two test sets. In the first test set, the effectiveness of the rock drillability index and drilling specific energy will be discussed by cutting rocks with different depths. The second test set can study whether the heterogeneity of rock will affect the accuracy of these two methods. The cutting depth of the rock models generated in the numerical model are respectively 2mm, 2.6mm, 3.2mm

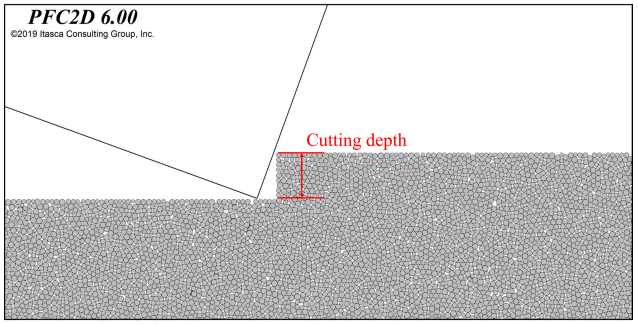

FIGURE 6. Interaction between particles and PDC cutter.

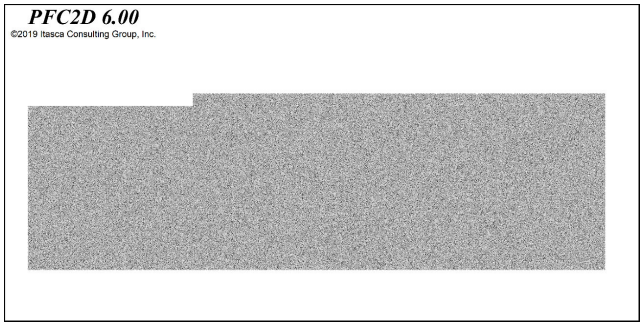

FIGURE 7. Rock model for linear cutting.

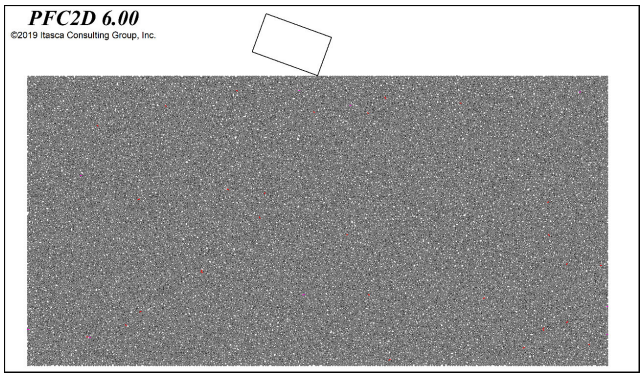

FIGURE 8. Rock model for vertical pressing-in.

and 4.5mm. To ensure that the PDC cutter can contact and interact with at least five rows of particles during cutting process, as illustrated in **Figure 6**, the diameter of particles is specified to be 0.3–0.5mm. To minimize the boundary effect, the dimensions of the model is set to 20 × 70mm, as shown in **Figure 7**, making the entire model contains approximately 60,000 particles. Similarly, the diameter of the particles in the model of vertical rock pressing-in is specified to be 0.3–0.5mm, and the dimensions of the model is set to 20×40mm, as illustrated in **Figure 8**. The number of particles contained in the whole model is about 33,000. In addition, to simulate the effect of ground stress, a lateral pressure of 10MPa was added to both sides of the above two models through servo control.

C. CALIBRATION OF MESOSCOPIC PARAMETERS FOR THE ROCK MODEL

After modelling, the mesoscopic parameters of the above models need to be determined. As described before, the particle bonding method in PFC^{2D} relies on a series of bonds between particles. It is necessary to calibrate the mesoscopic parameters of bonds through uniaxial tests so that the rock model can reflect the physical and mechanical properties of the real rock. Researchers usually choose the stress-strain curve obtained from the laboratory uniaxial compression test as a reference and use the 'test and error' method, which is illustrated in **Figure 9** for Unconfined Compressive Strength (UCS) test, to calibrate the mesoscopic parameters of rock model until the simulated curve and failure mode are basically consistent with the experiment [43], [45], [46].

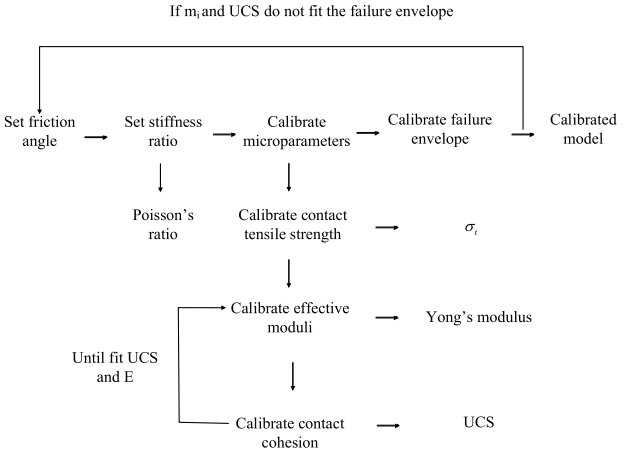

FIGURE 9. The 'trial and error' method for parameter checking process of PFC model [45].

To achieve the above objectives, a series of standard cylindrical specimens with dimensional parameters of 100 × 50mm was poured. Then the uniaxial tests were performed on the rock test machine 815 (MTS815) to obtain the referenced stress-strain curve and failure mode of poured specimens. Meanwhile, the rock models with the particle diameter of 0.3–0.5mm and the dimensional parameters of 100 × 50mm were generated for the uniaxial simulating test. As shown in **Figure 10**, the entire model contains approximately 35,000 particles.

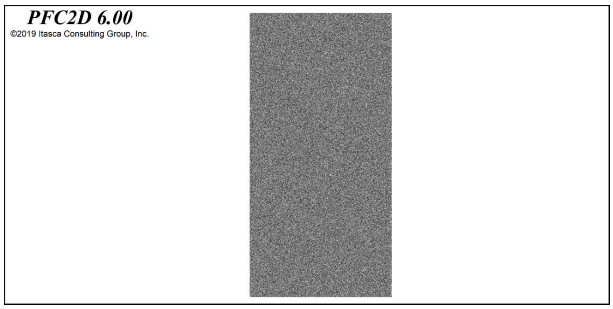

FIGURE 10. Rock model for uniaxial simulating tests.

The actual rock is a heterogeneous solid aggregate. To give the numerical model the heterogeneity of the actual rock, it is assumed that the mesoscopic parameters of the model conform to the Weibull distribution, which is defined by the **Equation (1)**:

$$f(u) = \frac{m}{u_0}\left(\frac{u}{u_0}\right)^{m-1} \exp\left(-\frac{u}{u_0}\right)^{m} \quad (1)$$

where u is the parameter of each element (such as internal friction angle and cohesion), the proportional parameter u_0 is related to the average value of each element, and the m define the shape of the distribution function. For Weibull distribution, the value of m must be greater than zero, so $m = 5$ and $m = 2$ are used to analyze the influence of heterogeneity in this study [47]. After the Weibull distribution is assigned to the mesoscopic parameters of the rock models, this heterogeneous material generated by the computer can be used to simulate the real rock specimens used in the laboratory.

In both numerical and laboratory tests, the loading rates on the top and bottom are set to 0.002 mm/s. In the process of calibration of mesoscopic parameters, these parameters will be systematically changed according to the 'trial and error' method. The stress-strain curve will be obtained and checked whether it has macro characteristics after each simulation tests. This calibration process will be repeated until the mechanical response of the numerical model matches the mechanical response of the laboratory rock specimens. After the calibrating process is over, as shown in **Figure 11**, it is found that the stress-strain curve and failure mod obtained by experiment and simulation are basically the same (the relative error of peak stress and peak strain are 2.3% and 8.5%, respectively). Therefore, the results of laboratory and numerical simulation are matched in this study. However, the curves of simulation and experiment are slightly different in the pre-peak phase. Considering that the compaction stage of the rock cannot be simulated by the current numerical simulation software, and the elastic modulus of the rock is not the main research object of this study, then it can be considered that the calibrated parameters in **Table 1** and **Table 2** are appropriate.

TABLE 1. Mesoscopic parameters irrelevant to heterogeneity and strength of rock.

Parameters	Value
Minimum particle size (mm)	0.3
Maximum particle size(mm)	0.5
Density (kg*m-3)	2500
Porosity	0.1
Contact bond modulus (GPa)	0.6
Contact bond stiffness ratio	1.0
Friction coefficient	0.7
Parallel bond friction angle (°)	40
Parallel bond modulus (GPa)	8.7
Parallel bond stiffness ratio	1

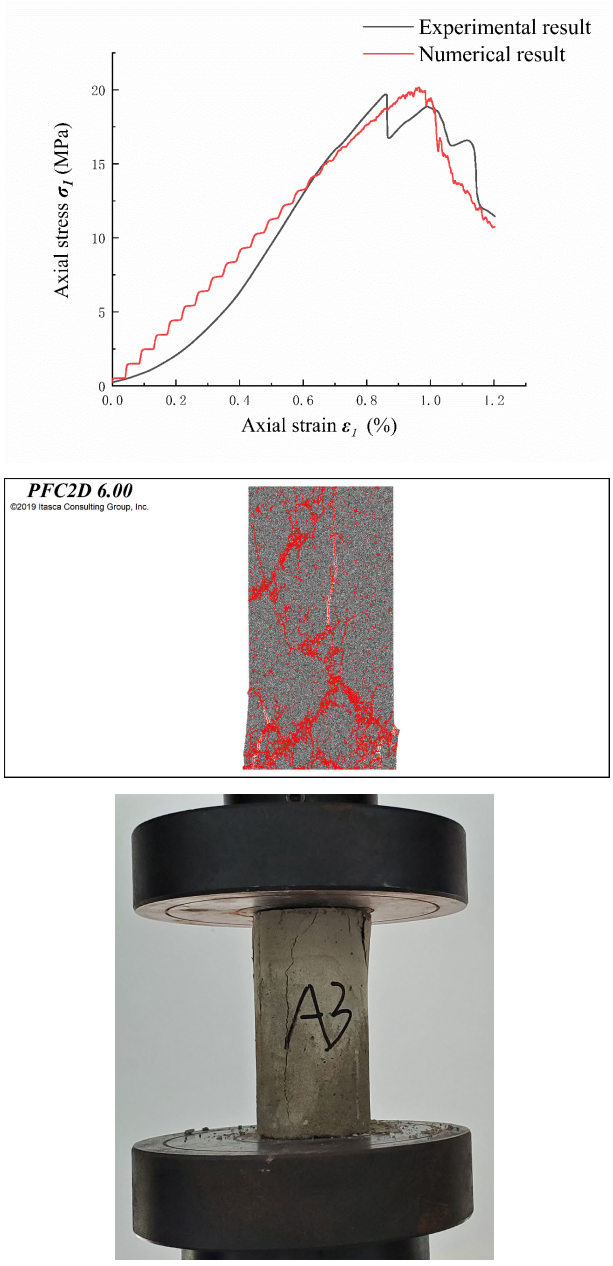

FIGURE 11. UCS result comparison between numerical simulation and laboratory test.

D. CONFIGURE OF NUMERICAL SIMULATION

The ultimate goal of this study is to determine the relationship between rock drillability index, drilling specific energy and rock strength, and analyze the influence of rock heterogeneity on these two rock strength assessment methods. Therefore, this work designed and carried out a series of numerical tests on processes of horizontal linear rock cutting and vertical rock pressing-in. As mentioned in **Section 2**, this study separately discusses the above two processes to simplify the numerical calculation [28], [34], [48] and obtains the mechanical parameters used to calculate the rock drillability index and drilling specific energy.

TABLE 2. Mesoscopic parameters relevant to heterogeneity and strength of rock.

Rock No.	Strength	heterogeneity coefficient	Parameters	Value (MPa)
A1	C20	2	Parallel bond tensile strength	25.8
			Parallel bond cohesion	30
A2		5	Parallel bond tensile strength	15.1
			Parallel bond cohesion	17.5
A3	C30	2	Parallel bond tensile strength	38.7
			Parallel bond cohesion	45
A4		5	Parallel bond tensile strength	22.36
			Parallel bond cohesion	26
A5	C40	2	Parallel bond tensile strength	52.5
			Parallel bond cohesion	61
A6		5	Parallel bond tensile strength	30.19
			Parallel bond cohesion	35.1

TABLE 3. Setting of parameters in horizontal linear rock cutting simulation with weaker heterogeneity.

Rock No.	UCS (MPa)	Test set	Cutting depth (mm)	Heterogeneity coefficient	Cohesion (MPa)
A2	20	1	2	5.0	17.5
		2	2.6		
		3	3.2		
		4	4.5		
A4	30	5	2	5.0	26
		6	2.6		
		7	3.2		
		8	4.5		
A6	40	9	2	5.0	35.1
		10	2.6		
		11	3.2		
		12	4.5		

To verify the feasibility of rock drillability index and drilling specific energy, three sets of simulation tests of horizontal linear rock cutting have been carried out. The rock models used in horizontal linear rock cutting are specified with different cutting depths, strengths and heterogeneity. Firstly, the vertical rock pressing-in tests were carried out on the C20, C30 and C40 rock models with weak heterogeneity to obtain the relationship between the normal force and the cutting depth. Subsequently, horizontal linear rock cutting tests were performed on these three kinds of rocks, and the parameter settings are shown in **Table 3**.

On the other hand, to analyze whether rock heterogeneity will affect the accuracy of rock drillability index and drilling specific energy when drilling rocks with same uniaxial strength, this study designed three sets of simulation tests of horizontal linear rock cutting, which contains rock models with different cutting depths, strengths and same higher heterogeneity. Firstly, the vertical rock pressing-in tests were carried out on the C20, C30 and C40 rock models with higher heterogeneity to obtain the relationship between the normal force and the cutting depth. Subsequently, horizontal linear rock cutting tests were performed on these three kinds of rocks, and the parameter settings are shown in **Table 4**.

IV. SIMULATION RESULTS AND DISCUSSION

The force signal processing procedures used to further calculate the rock drillability index and drilling specific energy in the numerical simulation, along with the applicability evaluation of rock drillability index and drilling specific energy, will be addressed in this section.

A. ROCK DRILLABILITY INDEX AND DRILLING SPECIFIC ENERGY FOR SINGLE PDC CUTTER

As stated in **Section 1**, rock drillability index and drilling specific energy are obtained based on in-situ tests, while, this work is to study the rock breaking process by a single PDC cutter, it is necessary to simplify these two rock strength assessment methods.

TABLE 4. Setting of parameters in horizontal linear rock cutting simulation with weaker heterogeneity.

Rock No.	UCS (MPa)	Test set	Cutting depth (mm)	Heterogeneity coefficient	Cohesion (MPa)
A1	20	13	2	2.0	30
		14	2.6		
		15	3.2		
		16	4.5		
A3	30	17	2	2.0	45
		18	2.6		
		19	3.2		
		20	4.5		
A5	40	21	2	2.0	61
		22	2.6		
		23	3.2		
		24	4.5		

In previous studies, rock drillability index was used to make preliminary assessments on the geological conditions of the surrounding rock of the roadway. But past researchers have not specifically assessed rock strength by using the rock drillability index. The rock drillability index was proposed based on dimensionless analysis theory as follows:

$$I_d = \gamma \pi_1^{\alpha} \pi_2^{\beta} \tag{2}$$

where γ, α and β are parameters that need to be obtained by fitting results of in-situ tests. According to previous study [9], [49], the value of γ, α and β are determined as 1, 1, and 0.4 respectively. The two dimensionless parameters π_1 and π_2 are defined as follows:

$$\begin{cases} \pi_1 = \dfrac{DF_P}{M}, \\ \pi_2 = \dfrac{v}{D\omega}, \end{cases} \tag{3}$$

where D is the diameter of the borehole, F_P is the pushing force against the bottom of the borehole, M is the torque on the drill bit, v is the penetration velocity and ω is the rotation speed of the drill bit. Since the simulation of horizontal linear rock cutting by single PDC cutter cannot obtain the angular velocity, torque, drilling speed and other parameters of the drill bit required by calculation rock drillability index, this study simplified the formula to make it conform to calculation mode for the single PDC cutter.

Firstly, assuming that the penetration velocity of the drill bit is constant, that is, the drilling distance within Δt is d. The penetration velocity can be obtained by **Equation (4)**:

$$v = \frac{d}{\Delta t} \tag{4}$$

Since the diameter of borehole is D, the torque M can be converted into **Equation (5)**:

$$M = \sum_1^n F_{SC} \cdot r \tag{5}$$

where F_{SC} is the cutting force acting on the single PDC cutter, n is number of cutters of the drill bit and r is the distance between a cutter and the centre of the drill bit. This study only concentrates on single PDC cutter, so take the cutter on the outer ring of the drill bit for research, that is $r = \frac{D}{2}$. Meanwhile, assuming that the time consumed for one revolution of the drill bit is Δt, the angular velocity can be obtained by **Equation (6)**:

$$\omega = \frac{2\pi}{\Delta t} \tag{6}$$

Then substituting **Equation (4)**, **(5)** and **(6)** into **Equation (1)** can obtain the rock drillability index for single PDC cutter as follows:

$$I_d = \frac{2F_{SP}}{F_{SC}} \left(\frac{d}{2\pi D} \right)^{0.4} \tag{7}$$

where d is cutting depth, which will change according to the change of penetration velocity. F_{SP} and F_{SC} are the vertical and cutting force acting on the single PDC cutter respectively.

Teale proposed a method for determining rock strength by using the energy consumed by the drill bit during the drilling process [10]. This method is generally regarded as a standard method for determining rock strength, and many scholars had further developed it [50]–[52]. However, none of them has changed Teale's core idea, that is, the energy consumed by the drilling bit during drilling process can be divided into energy consumed by the process of thrust pushing the drill bit forward and the energy consumed by the rotary rock cutting. In this method, Teale proposed drilling specific energy e based on drilling parameters as follows:

$$e = \left(\frac{F_P}{A} \right) + \left(\frac{2\pi}{A} \right) \left(\frac{MN}{v} \right) \tag{8}$$

where N is rotation speed. By using the subscript t and r to represent the 'thrust' and 'rotary' components respectively, the components of drilling specific energy e can be

expressed as:

$$e_t = \left(\frac{F_P}{A}\right) \tag{9}$$

$$e_r = \left(\frac{2\pi}{A}\right)\left(\frac{NM}{v}\right) \tag{10}$$

During drilling process, the diameter of drill bit is constant, so e_t is proportional to F_P. In most cases, compared to e_r, e_t is very small and can be neglected [10]. Therefore, this study mainly simplified e_r to make it conform to the calculation mode of single PDC cutter. Substituting **Equation (4)**, **(5)** and **(6)** into **Equation (10)** can obtain the drilling specific energy for single PDC cutter as follows:

$$e_r = \left(\frac{4}{D}\right)\left(\frac{F_{SC}}{d}\right) \tag{11}$$

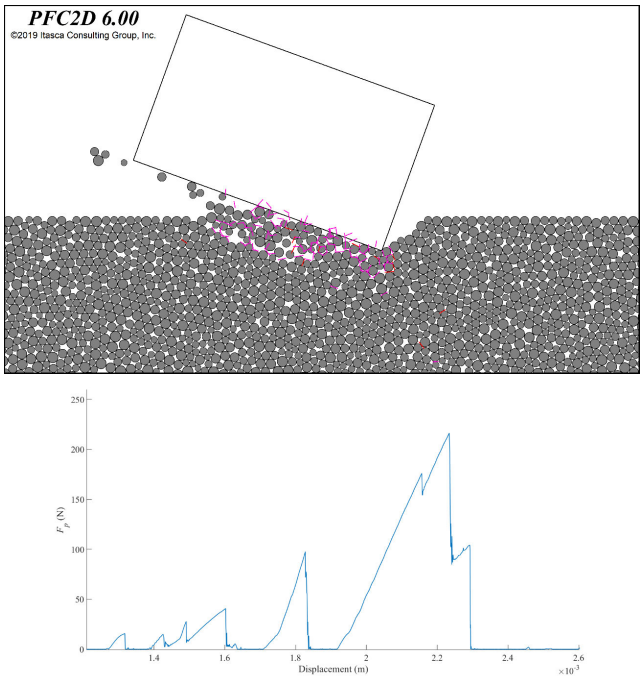

FIGURE 12. Process of slag discharge and normal force drop.

B. NORMAL FORCE PROCESSING

In the actual drilling process, rock breaking process by the rotation of PDC drill bit is a continuous process, so the normal force acting on the single PDC cutter should have a certain proportional relationship with the cutting depth. However, as described in **Section 2(B)**, vertical rock pressing-in is a discontinuous cyclic failure process, including rock destruction (the maximum normal force acting on the cutter will be obtained in this stage) and slag discharge. **Figure 12** illustrates the process of PDC cutter pressing into the rock to discharge slag and normal force drop, but considering the actual drilling process stated previously, the process of discharging of rock chips was not taken into account in the calculation by this study, that is, the normal force acting on the cutter and cutting depth satisfies the linear relation **Equation (12):**

$$F_{SP} = kd \tag{12}$$

where k is the proportional coefficient of normal force and cutting depth, which changes with the strength of rock models.

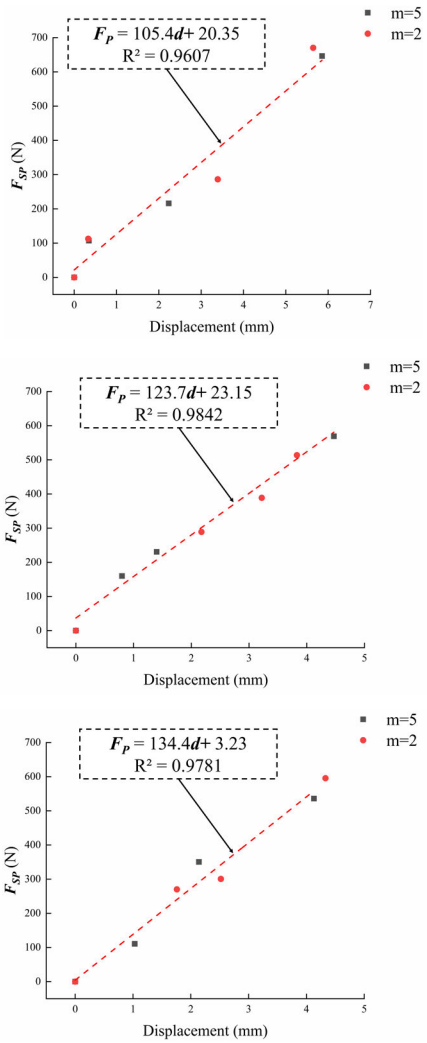

FIGURE 13. Scatter diagram of the relationship between normal force and displacement.

The numerical simulation results of vertical rock pressing-in are shown in **Figure 13**, regardless of the rock's heterogeneity, as long as the uniaxial strength remains unchanged, the ratio of the normal force to the cutting depth will not change significantly.

C. CUTTING FORCE PROCESSING

In order to obtain the cutting force, this study monitors the force acting on a single PDC cutter. As mentioned in **Section 2(B)**, in PFC^{2D} software, rock particles will be broken when they encounter the cutting face of the PDC cutter

TABLE 5. Average value of peak cutting forces determined from numerical simulation.

UCS (MPa)	Heterogeneity coefficient	Cutting depth (mm)	Average value of peak cutting force (N)
20	5	2	117.27
		2.6	171.87
		3.2	234.87
		4.5	365.11
	2	2	123.70
		2.6	176.40
		3.2	226.87
		4.5	370.74
30	5	2	192.48
		2.6	291.89
		3.2	380.06
		4.5	614.58
	2	2	195.97
		2.6	281.44
		3.2	395.21
		4.5	617.75
40	5	2	266.78
		2.6	392.17
		3.2	534.92
		4.5	843.23
	2	2	264.82
		2.6	370.18
		3.2	529.31
		4.5	823.13

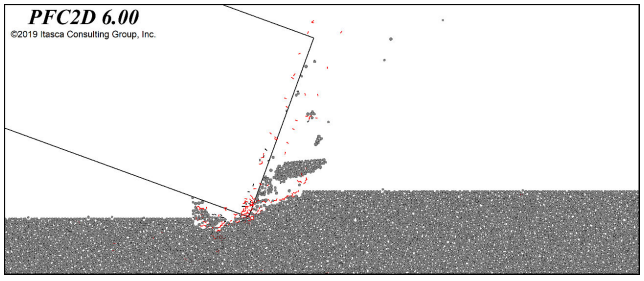

FIGURE 14. Breaking process of rock under peeling surface by PDC cutter.

and reach a predetermined tensile stress level. Then the cutter will cut the remaining rock particles below the peeling surface, as shown in **Figure 14**, making a large number of tiny cutting forces generated after the peak cutting force appears. However, these tiny cutting forces should be ignored to avoid affecting the obtainment of the actual cutting force. To improve the reliability of the numerical simulation, this study performed the following process on the cutting force output by the PFC^{2D}: take the peak cutting force during each complete cycle of the horizontal linear rock cutting mentioned in **Section 2(B)**, and the actual cutting force used for calculation is the average of all peak cutting forces [53], [54]. The cutting force used to calculate rock drillability index and drilling specific energy is average value of all peak cutting force in the X-direction, and **Figure 15** illustrates that peak cutting force collected in rock model with cutting depth $d = 2$ mm and heterogeneity coefficient $m = 5$. It should be noted that the peak cutting forces have certain volatility, which can be reflected from the volume of the rock chips in **Figure 15**, that is, the larger the volume of the rock chips being cut, the greater the required peak cutting force. The average value of the processed peak cutting forces is shown in **Table 5**.

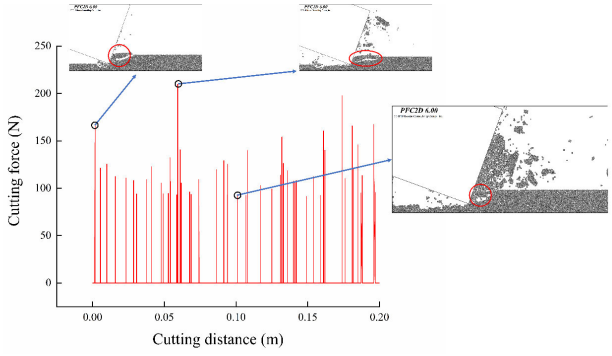

FIGURE 15. Cutting force and chip formation determined from numerical simulations.

D. APPLICATION OF ROCK DRILLABILITY INDEX AND DRILLING SPECIFIC ENERGY FOR ROCK WITH SAME HETEROGENEITY

In this study, two sets of horizontal linear rock cutting tests and their corresponding vertical rock pressing-in tests have been carried out. For simplicity, the statistical results of rock drillability index and drilling specific energy of rock models with same heterogeneity will be classified and discussed in this section. The purpose of this study is to reveal the reliability of rock drillability index for rock strength assessment and make a preliminary comparison with drilling specific energy.

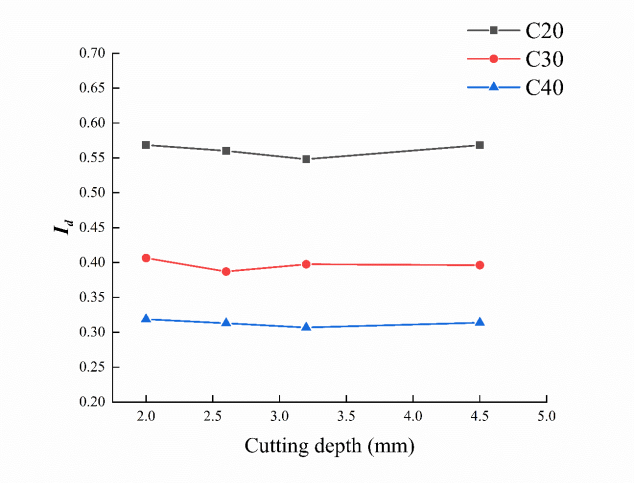

FIGURE 16. The average value of I_d with different cutting depth for three kinds of rock with same heterogeneity coefficient of 5.

As shown in **Figure 16**, the average values of rock drillability index during horizontal linear rock cutting process of rock models with different strength and same heterogeneity coefficient of 5 at four different cutting depths were plotted. It can be seen that the average value of rock drillability index did not change significantly with cutting depth of the same kind of rock. Since the change of the cutting depth can reflect the change of drilling speed, as stated in **Section 4(A)**, the above results can indicate that the drillability index of the rock with same strength will no fluctuate greatly, no matter how the drilling speed changes during the actual drilling process [9]. Besides, the value of rock drillability index continues to decrease as the strength of the rock continues to increase, so the following results can be deduced: the harder the rock, the smaller value of I_d, which also in line with the results of the research done by the former scholar [9].

On the other hand, As shown in **Figure 17**, the average values of drilling specific energy during horizontal linear rock cutting process of rock models with different strength and same heterogeneity coefficient of 5 at four different cutting depths were plotted. It can be seen that the average value of drilling specific energy will slightly increase as the cutting depth increases. In this study, it is considered that increment in the cutting depth means increasing the penetration velocity, as illustrated in **Section 4(A)**, while

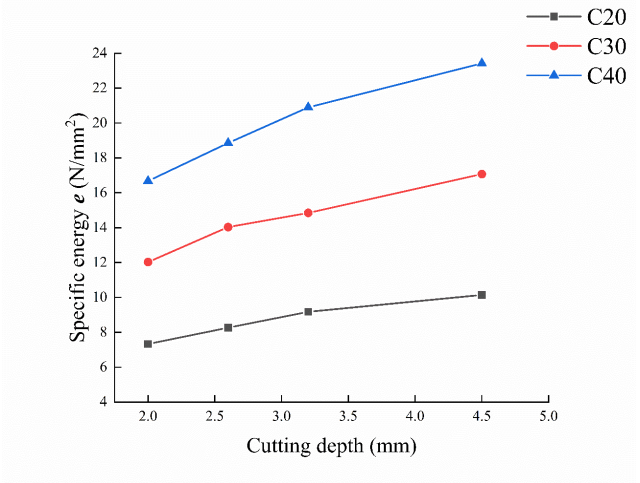

FIGURE 17. The average value of e with different cutting depth for three kinds of rock with same heterogeneity coefficient of 5.

increasing the penetration velocity in the actual drilling process requires increasing the pushing force. Therefore, the results in **Figure 17** are in line with Teale's research results, that is, when the pushing force is increased to a certain extent, the efficiency of rock breaking will decrease, leading to the increment of drilling specific energy [10]. It is noteworthy that as the strength of the rock increases, the energy required to break the rock will also increase.

By comparing the specific energy of drilling specific energy with rock drillability index, it can be found that no matter how the cutting depth changes, the rock drillability index can be maintained at the same level. On the contrary, drilling specific energy will change to a certain extent, which lead to errors in rock strength assessment, and the detailed comparison of these two methods will be introduced latter.

E. EFFECT OF ROCK HETEROGENEITY ON ROCK DRILLABILITY INDEX AND DRILLING SPECIFIC ENERGY

Natural rock mass has certain heterogeneity since there are various defects in it. In **Section 4(D)**, the applicability of rock drillability index and drilling specific energy under the condition of good rock homogeneity has been discussed mainly. Therefore, in this section, emphasis will be placed on whether heterogeneity affects the accuracy of the above two methods.

As shown in **Figure 18** and **Figure 19**, the average values of rock drillability index and drilling specific energy with different heterogeneity during horizontal linear rock cutting have been plotted separately. It can be found that the difference in the rock heterogeneity will not affect the rock drillability index and the drilling specific energy, as long as the rock strength is kept constant. This indicates that the rock drillability index and drilling specific energy have good environmental adaptability, making these two methods capable of assessing the rock strength regardless of rock heterogeneity. In addition, as shown in **Figure 19**, it also can be seen that

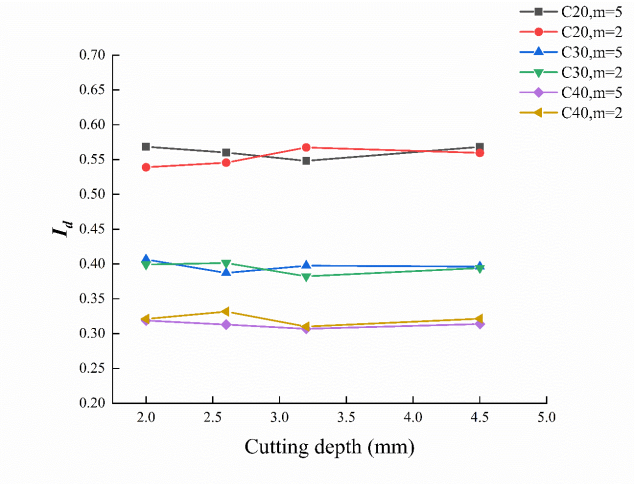

FIGURE 18. Comparison of average values of rock drillability index with different heterogeneity.

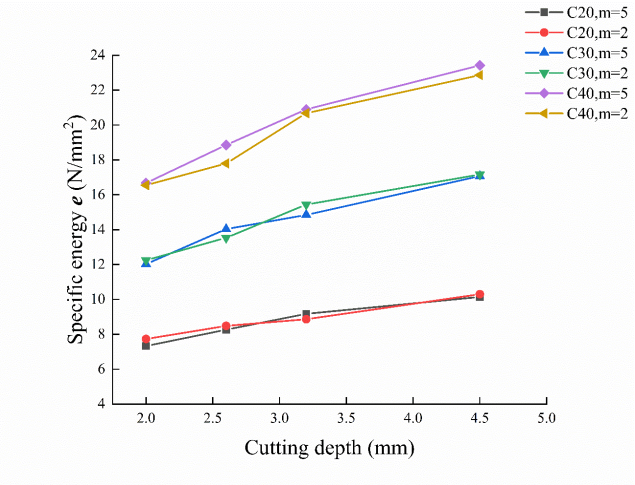

FIGURE 19. Comparison of average values of drilling specific energy with different heterogeneity.

the drilling specific energy conforms to the conclusion in **Section 4(D)**, that is, drilling specific energy will have a certain change with the change of cutting depth.

From the above analysis, it can be concluded that changes in rock heterogeneity will not affect the use of rock drillability index and drilling specific energy to assess the rock strength. Therefore, this study believes that these two methods can be used to predict rock strength. **Figure 20** shows a scatter diagram of the relationship between rock drillability index and rock strength, which was plotted based on the average value of I_d during horizontal linear rock cutting simulation. An equation describing the relationship between I_d and UCS is obtained by linear regression fit analysis:

$$\mathrm{UCS} = 0.012I_d + 0.783 \tag{13}$$

On the other hand, **Figure 21** illustrates a scatter diagram of the relationship between e and UCS that was plotted based on the average value of e during horizontal linear rock cutting

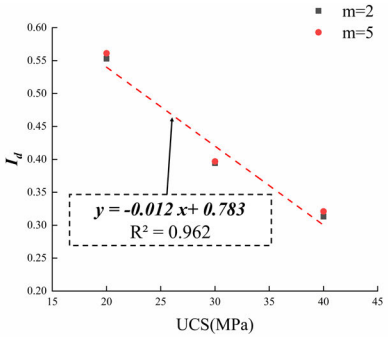

FIGURE 20. Relationship between UCS and the rock drillability index.

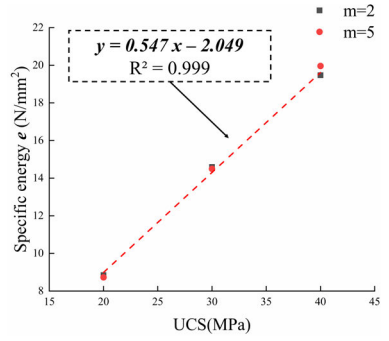

FIGURE 21. Relationship between UCS and the drilling specific energy.

simulation. An equation describing the relationship between e and UCS is obtained by linear regression fit analysis. Overall, e increases with increasing UCS in a linear form (**Equation (14)**).

$$\mathrm{UCS} = 0.547e - 2.049 \tag{14}$$

F. COMPARISON OF THE ACCURACY OF ROCK DRILLABILITY INDEX AND DRILLING SPECIFIC ENERGY

At present, drilling specific energy is a mainstream method to assess rock strength while drilling. However, according to **Section 4(D)**, it can be known that drilling specific energy has certain limitations. Therefore, it is more reliable to use the drillability index to assess the rock strength.

To more intuitively compare the advantages and disadvantages between rock drillability index and drilling specific energy, the average value and error of rock drillability index and drilling specific energy are calculated and shown in **Figure 22**. It can be found that there will not be large errors by using the rock drillability index to assess rock strength, and the rock strength can be obtained accurately. On the contrary, the average value of drilling specific energy can reflect the change of rock strength, but the error is large, making the effect of applying it to the actual rock strength evaluation is relatively bad. On the other hand, by comparing the error of rock drillability index and drilling specific energy, it is found that the error of the former is smaller than that of the latter,

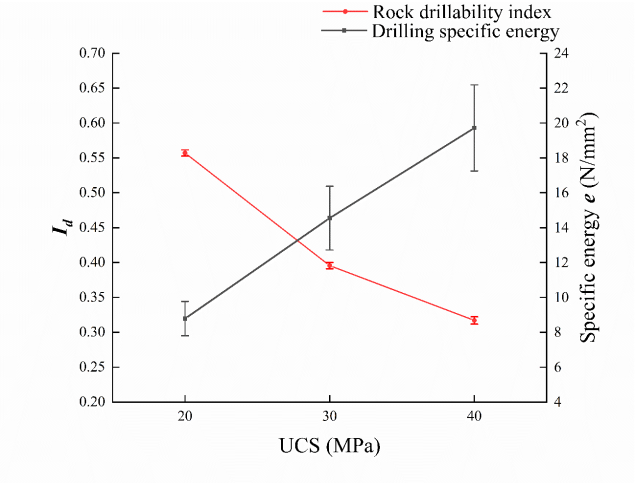

FIGURE 22. Relationship between UCS and the drilling specific energy.

which indicates that the rock drillability index is better than the drilling specific energy in assessment of rock strength.

In this paper, the actual drilling process of a complete drill bit is simplified into an analysis of rock breaking process with a single PDC cutter [53], [54]. Although the value of the simulated results may be slightly different from the real-world application, the feasibility of these two methods (Rock drillability index and drilling specific energy) can be discussed qualitatively through numerical simulation of rock breaking mechanics by single PDC cutter. Accurate quantitative analysis about the applicability of the above two methods through the rock breaking process of a single PDC cutter needs to be further explored by laboratory tests which will be carried out by designing a novel single PDC cutter rock breaking equipment in the follow-up research.

V. CONCLUSION

To analyze the feasibility of rock drillability index and drilling specific energy in assessing rock strength and compare the advantages and disadvantages of these two methods, novel numerical experiments are performed based on PFC^{2D}. The findings of this research are summarized as follows:

(1) Through the analysis of simulation results, it can be found that although the cutting depth has changed, the rock drillability index is maintained in a relatively stable range without large fluctuations when cutting rocks with same strength. The rock drillability index keeps decreasing with the increase of rock strength following a linear form.

(2) In the process of horizontal linear rock cutting, as the cutting depth increases, the drilling specific energy has a slight upward trend. This phenomenon can indicate that an increase in thrust (indicated by the increment of cutting depth) to a certain extent will reduce the efficiency of rock breaking, which in turn will increase the drilling specific energy. But from the statistical analysis of the simulation results, the drilling specific energy increases as the strength of the rock increases following a linear form.

(3) Under the condition that the uniaxial strength of the rock remains unchanged, the heterogeneity of the rock will not affect the use of rock drillability index and drilling specific energy to evaluate the rock strength. This suggests that these two methods have good environmental adaptability, which can be used to assess rock strength regardless of rock type.

(4) By comparing the error of the rock drillability index with that of the drilling specific energy, it can be found that the error of the drilling specific energy is greater than that of the rock drillability index. Therefore, the rock drillability index superior to drilling specific energy is suggested for rock strength assessment.

REFERENCES

[1] U. Ahmed, D. Bordelon, and D. Allen, "MWD rock mechanical properties to avoid drilling related problems," in *Proc. SPE/IADC Drilling Conf.*, 1993, p. 7, doi: 10.2118/25692-MS.

[2] M. Löfgren and I. Neretnieks, "Formation factor logging by electrical methods: Comparison of formation factor logs obtained in situ and in the laboratory," *J. Contam. Hydrol.*, vol. 61, no. 1, pp. 107–115, 2003, doi: 10.1016/S0169-7722(02)00117-1.

[3] G. El-Qady, M. Hafez, M. A. Abdalla, and K. Ushijima, "Imaging subsurface cavities using geoelectric tomography and ground-penetrating radar," *J. Cave Karst Stud.*, vol. 67, pp. 174–181, Dec. 2005.

[4] A. K. Benson, "Applications of ground penetrating radar in assessing some geological hazards: Examples of groundwater contamination, faults, cavities," *J. Appl. Geophys.*, vol. 33, no. 1, pp. 177–193, 1995, doi: 10.1016/0926-9851(95)90040-3.

[5] M. Bakalowicz, "La zone d'infiltration des aquifères karstiques. Méthodes d'étude, "Structure et fonctionnement," *Hydrogéologie*, vol. 4, pp. 3–21, Jan. 1995.

[6] M. Beres, M. Luetscher, and R. Olivier, "Integration of ground-penetrating radar and microgravimetric methods to map shallow caves," *J. Appl. Geophys.*, vol. 46, no. 4, pp. 249–262, 2001, doi: 10.1016/S0926-9851(01)00042-8.

[7] M. R. J. Wyllie, A. R. Gregory, and L. W. Gardner, "Elastic wave velocities in heterogeneous and porous media," *Geophysics*, vol. 21, no. 1, pp. 41–70, Jan. 1956, doi: 10.1190/1.1438217.

[8] Q. Shi, M. Liu, X. Liu, P. Liu, P. Zhang, J. Yang, and X. Li, "Domain adaption for fine-grained urban village extraction from satellite images," *IEEE Geosci. Remote Sens. Lett.*, vol. 17, no. 8, pp. 1430–1434, Aug. 2020, doi: 10.1109/LGRS.2019.2947473.

[9] K. Zhang, R. Hou, G. Zhang, G. Zhang, and H. Zhang, "Rock drillability assessment and lithology classification based on the operating parameters of a drifter: Case study in a coal mine in China," *Rock Mech. Rock Eng.*, vol. 49, no. 1, pp. 329–334, Feb. 2015, doi: 10.1007/s00603-015-0723-0.

[10] R. Teale, "The concept of specific energy in rock drilling," *Int. J. Rock Mech. Min. Sci. Geomech. Abstr.*, vol. 2, no. 1, pp. 57–73, 1965, doi: 10.1016/0148-9062(65)90022-7.

[11] L. L. Mishnaevsky, "Physical mechanisms of hard rock fragmentation under mechanical loading: A review," *Int. J. Rock Mech. Min. Sci. Geomech. Abstr.*, vol. 32, no. 8, pp. 763–766, 1995, doi: 10.1016/0148-9062(95)00027-E.

[12] I. Evans, *A Theory of the Basic Mechanics of Coal Ploughing*. Columbia, MO, USA: The Curators of the Univ. Missouri, 1962.

[13] M. Hood and H. Alehossein, "A development in rock cutting technology," *Int. J. Rock Mech. Min. Sci.*, vol. 37, no. 1, pp. 297–305, 2000, doi: 10.1016/S1365-1609(99)00107-0.

[14] R. M. Goktan and N. G. Yilmaz, "A new methodology for the analysis of the relationship between rock brittleness index and drag pick cutting efficiency," *J. South Afr. Inst. Min. Metall.*, vol. 105, no. 10, pp. 727–732, 2005.

[15] K. Liu, X. P. Li, and S. Y. Liang, "The mechanism of ductile chip formation in cutting of brittle materials," *Int. J. Adv. Manuf. Technol.*, vol. 33, nos. 9–10, pp. 875–884, Jun. 2007, doi: 10.1007/s00170-006-0531-5.

[16] Y. Nishimatsu, "The mechanics of rock cutting," *Int. J. Rock Mech. Mining Sci. Geomech. Abstracts*, vol. 9, no. 2, pp. 261–270, 1972, doi: 10.1016/0148-9062(72)90027-7.

[17] Y. Nishimatsu, M. Akiyama, S. Okubo, and T. Yoshida, "On the effect of rake angle of drag bit in rock cutting," *J. Mining Inst. Jpn.*, vol. 100, no. 1161, pp. 1063–1067, 1984, doi: 10.2473/shigentosozai1953.100.1161_1063.

[18] D. Che and K. F. Ehmann, "Polycrystalline diamond turning of rock," in *Proc. Int. Manuf. Sci. Eng. Conf.*, vol. 10, Jun. 2013, Art. no. V001T01A027, doi: 10.1115/MSEC2013-1127.

[19] D. Che and K. Ehmann, "Experimental study of force responses in polycrystalline diamond face turning of rock," *Int. J. Rock Mech. Mining Sci.*, vol. 72, pp. 80–91, Dec. 2014, doi: 10.1016/j.ijrmms.2014.08.014.

[20] C. J. Durrand, M. R. Skeem, R. B. Crockett, and D. R. Hall, "Superdard, thick, shaped PDC cutters for hard rock drilling: Development and test results," in *Proc. 25th Workshop Geothermal Reservoir Eng.*, 2010, pp. 1–8.

[21] D. Che, W.-L. Zhu, and K. F. Ehmann, "Chipping and crushing mechanisms in orthogonal rock cutting," *Int. J. Mech. Sci.*, vol. 119, pp. 224–236, Dec. 2016, doi: 10.1016/j.ijmecsci.2016.10.020.

[22] H. Çopur, H. Tunçdemir, N. Bilgin, and T. Dinçer, "Specific energy as a criterion for the use of rapid excavation systems in turkish mines," *Mining Technol.*, vol. 110, no. 3, pp. 149–157, Dec. 2001, doi: 10.1179/mnt.2001.110.3.149.

[23] Z. Wang, W. Wang, J. Wang, and C. Liu, "Cutting simulation and test based on different rock parameters," in *Proc. IEEE Int. Conf. Inf. Autom. (ICIA)*, Aug. 2013, pp. 735–740, doi: 10.1109/ICInfA.2013.6720391.

[24] J. Futo, F. Krepelka, and L. Ivanicova, "Optimization of rock cutting process using the simulation methods," in *Proc. 12th Int. Carpathian Control Conf. (ICCC)*, May 2011, pp. 120–122, doi: 10.1109/CarpathianCC.2011.5945829.

[25] X. Li and Y. Liang, "Finite element simulation and experiment study of high manganese steel drilling," in *Proc. ICCMS Int. Conf. Comput. Modeling Simulation*, vol. 1, Jan. 2010, pp. 54–58, doi: 10.1109/ICCMS.2010.152.

[26] X. Li, S. Wang, R. Malekian, S. Hao, and Z. Li, "Numerical simulation of rock breakage modes under confining pressures in deep mining: An experimental investigation," *IEEE Access*, vol. 4, pp. 5710–5720, 2016, doi: 10.1109/ACCESS.2016.2608384.

[27] X. Hu, C. Du, S. Liu, H. Tan, and Z. Liu, "Three-dimensional numerical simulation of rock breaking by the tipped hob cutter based on explicit finite element," *IEEE Access*, vol. 7, pp. 86054–86063, 2019, doi: 10.1109/ACCESS.2019.2925427.

[28] H. Geoffroy, D. Nguyen Minh, and C. Putot, "Study on interaction between rocks and worn PDC's cutter," *Int. J. Rock Mech. Min. Sci. Geomech. Abstr.*, vol. 34, nos. 3–4, p. 611, 1997, doi: 10.1016/S1365-1609(97)00036-1.

[29] Z. Tian, S. Jing, W. Liu, S. Gao, and J. Zhang, "Experimental and numerical study on cutting performance of coal plow," *IEEE Access*, vol. 8, pp. 211882–211891, 2020, doi: 10.1109/ACCESS.2020.3039438.

[30] J. Zou, W. Yang, and J. Han, "Discrete element modeling of the effects of cutting parameters and rock properties on rock fragmentation," *IEEE Access*, vol. 8, pp. 136393–136408, 2020, doi: 10.1109/ACCESS.2020.3011709.

[31] C. Yang, J. Hu, and S. Ma, "Numerical investigation of rock breaking mechanism with supercritical carbon dioxide jet by SPH-FEM approach," *IEEE Access*, vol. 7, pp. 55485–55495, 2019, doi: 10.1109/ACCESS.2019.2913172.

[32] Y. Weifeng, J. Yubing, S. Dingyi, and X. Xiaohong, "Discrete element numerical simulation of crack evolution in multi-coal seam mining," in *Proc. Int. Conf. Comput. Appl. Syst. Modeling (ICCASM)*, Oct. 2010, pp. 383–385, doi: 10.1109/ICCASM.2010.5622260.

[33] D. Che, W. Zhang, and K. Ehmann, "Chip formation and force responses in linear rock cutting: An experimental study," *J. Manuf. Sci. Eng.*, vol. 139, no. 1, Jan. 2017, Art. no. 011011, doi: 10.1115/1.4033905.

[34] T. Li, *Mechanical Analysis and Fragmentation Mechanism of PDC Bits Drilling Rock*. Wuhan, China: China Univ. Geosciences, 2012.

[35] M. E. Merchant, "Mechanics of the metal cutting process. II. Plasticity conditions in orthogonal cutting," *J. Appl. Phys.*, vol. 16, no. 6, pp. 318–324, Jun. 1945, doi: 10.1063/1.1707596.

[36] M. E. Merchant, "Mechanics of the metal cutting process. I. Orthogonal cutting and a type 2 chip," *J. Appl. Phys.*, vol. 16, no. 5, pp. 267–275, May 1945, doi: 10.1063/1.1707586.

[37] E. Detournay and P. Defourny, "A phenomenological model for the drilling action of drag bits," *Int. J. Rock Mech. Mining Sci. Geomech. Abstracts*, vol. 29, no. 1, pp. 13–23, Jan. 1992, doi: 10.1016/0148-9062(92)91041-3.

[38] M. Yahiaoui, J.-Y. Paris, K. Delbé, J. Denape, L. Gerbaud, and A. Dourfaye, "Independent analyses of cutting and friction forces applied on a single polycrystalline diamond compact cutter," *Int. J. Rock Mech. Mining Sci.*, vol. 85, pp. 20–26, May 2016, doi: 10.1016/j.ijrmms.2016.03.002.

[39] I. Rostamsowlat, B. Akbari, and B. Evans, "Analysis of rock cutting process with a blunt PDC cutter under different wear flat inclination angles," *J. Petroleum Sci. Eng.*, vol. 171, pp. 771–783, Dec. 2018, doi: 10.1016/j.petrol.2018.06.003.

[40] P. A. Cundall, "A computer model for simulating progressive large-scale movements in blocky rock systems," in *Proc. Int. Symp. Rock Mechanics*, vol. 1, 1971, pp. 11–18.

[41] P. A. Cundall and O. D. L. Strack, "A discrete numerical model for granular assemblies," *Géotechnique*, vol. 29, no. 1, pp. 47–65, Mar. 1979, doi: 10.1680/geot.1979.29.1.47.

[42] H. Shi, L. Song, H. Zhang, K. Xue, G. Yuan, Z. Wang, and G. Wang, "Numerical study on mechanical and failure properties of sandstone based on the power-law distribution of pre-crack length," *Geomech. Eng.*, vol. 19, no. 5, pp. 421–434, 2019, doi: 10.12989/gae.2019.19.5.421.

[43] X. Wang and L.-G. Tian, "Mechanical and crack evolution characteristics of coal–rock under different fracture-hole conditions: A numerical study based on particle flow code," *Environ. Earth Sci.*, vol. 77, no. 8, pp. 1–10, Apr. 2018, doi: 10.1007/s12665-018-7486-3.

[44] B. C. Storey, A. P. M. Vaughan, and T. R. Riley, "The links between large igneous provinces, continental break-up and environmental change?: Evidence reviewed from Antarctica," *Earth Environ. Sci. Trans. Royal Soc. Edinburg*, vol. 104, no. 1, pp. 17–30, 2020, doi: 10.1017/S175569101300011X.

[45] U. Castro-Filgueira, L. R. Alejano, J. Arzúa, and D. M. Ivars, "Sensitivity analysis of the micro-parameters used in a PFC analysis towards the mechanical properties of rocks," *Procedia Eng.*, vol. 191, pp. 488–495, Jan. 2017, doi: 10.1016/j.proeng.2017.05.208.

[46] S.-Q. Yang, Y.-H. Huang, H.-W. Jing, and X.-R. Liu, "Discrete element modeling on fracture coalescence behavior of red sandstone containing two unparallel fissures under uniaxial compression," *Eng. Geol.*, vol. 178, pp. 28–48, Aug. 2014, doi: 10.1016/j.enggeo.2014.06.005.

[47] W. C. Zhu and C. A. Tang, "Micromechanical model for simulating the fracture process of rock," *Rock Mech. Rock Eng.*, vol. 37, no. 1, pp. 25–56, Feb. 2004, doi: 10.1007/s00603-003-0014-z.

[48] H. Geoffroy, D. N. Minh, H. Maitournam, J. Bergues, and C. Putot, "Evaluation of drilling parameters of a PDC bit," in *Advances in Rock Mechanics*. Singapore: World Scientific, 1998, pp. 301–314.

[49] G. Niu, K. Zhang, B. Yu, Y. Chen, Y. Wu, and J. Liu, "Experimental study on comprehensive real-time methods to determine geological condition of rock mass along the boreholes while drilling in underground coal mines," *Shock Vibrat.*, vol. 2019, pp. 1–17, Nov. 2019, doi: 10.1155/2019/1045929.

[50] K. O. Hakalehto, "Energy required to break rock by percussive drilling," presented at the 14th U.S. Symp. Rock Mech. (USRMS), University Park, PA, USA, Jun. 11, 1972.

[51] O. Oloruntobi and S. Butt, "Application of specific energy for lithology identification," *J. Petroleum Sci. Eng.*, vol. 184, Jan. 2020, Art. no. 106402, doi: 10.1016/j.petrol.2019.106402.

[52] R. C. Pessier and M. J. Fear, "Quantifying common drilling problems with mechanical specific energy and a bit-specific coefficient of sliding friction," in *Proc. SPE Annu. Tech. Conf. Exhib.*, Jan. 1992, pp. 373–388, doi: 10.2118/24584-ms.

[53] J.-W. Cho, S. Jeon, S.-H. Yu, and S.-H. Chang, "Optimum spacing of TBM disc cutters: A numerical simulation using the three-dimensional dynamic fracturing method," *Tunnelling Underground Space Technol.*, vol. 25, no. 3, pp. 230–244, May 2010, doi: 10.1016/j.tust.2009.11.007.

[54] O. Su and N. A. Akcin, "Numerical simulation of rock cutting using the discrete element method," *Int. J. Rock Mech. Mining Sci.*, vol. 48, no. 3, pp. 434–442, 2011, doi: 10.1016/j.ijrmms.2010.08.012.

BOSONG YU is currently pursuing the master's degree in engineering mechanics with the China University of Mining and Technology, Xuzhou, China. His research interests include the rock mechanics and information recognition while drilling.

KAI ZHANG received the Ph.D. degree in geotechnical engineering from the Institute of Rock and Soil Mechanics, Chinese Academy of Sciences, Wuhan, China, in 2010.

He is currently a Professor with the State Key Laboratory for Geomechanics and Deep Underground Engineering, China University of Mining and Technology. He is also the Head of the Department of Mechanics and Engineering Science. His research interests include rock mechanics, underground engineering, coal mine roadway support, information recognition while drilling, and application of TBM in coal mines.

GANGGANG NIU is currently pursuing the Ph.D. degree in geotechnical engineering with the China University of Mining and Technology, Xuzhou, China. His research interests include the rock mechanics and information recognition while drilling.